Pergamon

Available online at www.sciencedirect.com
SCIENCE DIRECT®

Cement and Concrete Research 34 (2004) 1873–1879

CEMENT AND CONCRETE RESEARCH

Elaboration and thermal study of iron–phosphorus-substituted dicalcium silicate phase

My.Y. Benarchid[a,b], A. Diouri[a], A. Boukhari[a], J. Aride[b], J. Rogez[c,*], R. Castanet[c]

[a]Laboratoire de Chimie du Solide Appliquée, LAF 501, Faculté des Sciences, B.P. 1014. R.P.-Avenue Ibn Battouta, 10000 Rabat, Morocco
[b]Laboratoire de Physico-Chimie des Matériaux, LAF 502, E.N.S. Takaddoum, BP.5118, 10000 Rabat, Morocco
[c]Laboratoire TECSEN, UMR 6122, CNRS-Université Aix Marseille III, Case 251, Avenue Escadrille Normandie-Niemen 13397 Marseille Cedex 20, France

Received 1 May 2002; accepted 30 January 2004

Abstract

In the present work, we examine the simultaneous effect of iron and phosphorus additions on the calcium carbonate decomposition in $CaCO_3$, SiO_2, Fe_2O_3 and P_2O_5 mixtures at the molar ratio $CaCO_3/SiO_2 = 2$. The formation of the dicalcium silicate Ca_2SiO_4 is also studied. The temperatures of the decarbonation and the enthalpy evolution during the heating of the mixtures are measured. The additions of Fe_2O_3 and P_2O_5 oxides decrease the onset temperature of the $CaCO_3$ decomposition. The energy consumption of decarbonation at about 835 °C is lowered when the dopant concentrations increase. Synthesized solid solutions are analyzed by X-ray diffraction (XRD) and scanning electron microscopy (SEM). The free-lime quantity is determined by chemical analysis. The mineralogical analysis at room temperature of the products of the reaction shows the presence of iron–phosphorus-doped β, α′ and α-C_2S modifications.

Keywords: Calorimetry; Thermal analysis; X-ray diffraction; Ca_2SiO_4; SEM

1. Introduction

The theoretical energy consumption during the formation of the industrial clinker at 1450 °C is about 1605 J/g of clinker [1]. The major part of this energy is consumed during the endothermic process of calcium carbonate decomposition in raw meal. One of the main aims of the cement industry is to reduce this energy consumption. Several authors have already studied the influence of minor elements that are present or added to the raw meal on the $CaCO_3$ decomposition and the formation of the clinker phases [2–10].

The dicalcium silicate Ca_2SiO_4 (C_2S) is one of the main components of the Portland cement. It constitutes 15 to 30 wt.% of clinker and presents five allotropic forms: α, α'_H, α'_L, β and γ [11,12]. The β form is metastable under 500 °C and is hydraulically active. On the contrary, the γ stable form at ambient temperature is inactive towards water reaction. The α, α'_H, α'_L forms are stabilized at room temperature by the incorporation in their structures of foreign ions [12–16]. In common Portland clinkers, the belite phase C_2S is generally in the β form at room temperature [6].

In the literature, few systematic studies are devoted to the energy behaviour of the dicalcium silicate formation from initial mixtures of calcium carbonate and quartz in the presence of specific elements such as iron and phosphorus.

Iron oxide Fe_2O_3 is considered as the main flux in the clinker manufacture. It reduces the clinkerisation temperature and activates the solid-state reactions [17]. Weisweiler et al. [18] studied the effect of Fe_2O_3 on the phase equilibrium in a $CaO–SiO_2$ system. They showed that the C_2S phase is predominant at temperatures ranging 1100–1400 °C. Above 1400 °C, $CaO.SiO_2$ (CS) or the glassy phase $CaO.2SiO_2$ (CS_2) is the main observed phase. Less quantities of $3CaO.2SiO_2$ (C_3S_2) and $3CaO.SiO_2$ (C_3S) are also present. Regourd [19] studied the distribution of minor elements in the calcium silicates of industrial clinkers. She indicated that the iron maximal concentration is ranging 1–1.3 wt.% in belite C_2S and 0.6 wt.% in alite C_3S.

The P_2O_5 effect on the stability of the calcium silicates in Portland clinker has already been investigated [20–24]. It has been shown that a high level of phosphorus inhibits the C_3S formation. Diouri et al. [25–27] showed that the substitution of SiO_4^{4-} by PO_4^{3-} ions stabilizes the high temperature forms α′ and α'_L-C_2S.

* Corresponding author. CNRS-Universite Aix Marseille III, Laboratorie TECSEN, UMR 6122 Case 251, Avenue Escadrille Normandie-Niemen, Marseille Cedex 20 13397, France. Tel: +33-491-282-887; fax: +33-491-282-886.
E-mail address: j.rogez@univ.u-3mrs.fr (J. Rogez).

0008-8846/$ – see front matter © 2004 Elsevier Ltd. All rights reserved.
doi:10.1016/j.cemconres.2004.01.030

In this paper, we investigate the simultaneous influence of iron and phosphorus inclusions on the $CaCO_3$ decarbonation and the C_2S formation in $CaCO_3-SiO_2$ mixtures around the molar ratio $CaCO_3/SiO_2=2$. The decarbonation temperature is measured by differential thermal analysis. The enthalpy variations of the reaction at various temperatures are carried out by isothermal calorimetry. The synthesized solid solutions are characterized by X-ray diffraction (XRD) and scanning electron microscopy (SEM). Free lime is determined by chemical analysis.

2. Experimental

The starting materials are $CaCO_3$ provided by UCB (Brussels, Belgium), SiO_2, Fe_2O_3 and $(NH_4)_2HPO_4$ by Merck (Darmstadt, Germany) with >99% purity. They are ground in an agate mortar with ethanol as dispersive medium. The chemical reaction for the synthesis can be written as:

$$(2-2x)CaCO_3+(1-x)SiO_2+x/2Fe_2O_3+x(NH_4)_2HPO_4 \rightarrow (Ca_{2-2x}Fe_x\square_x)(Si_{1-x}P_x)O_4+(2-2x)CO_2\uparrow + 2xNH_3\uparrow+3x/2H_2O\uparrow$$

□: Cationic vacancy of Ca^{2+}.

Stoechiometric mixtures for $0\le x\le 0.20$ are the subject of the present investigation. They are as quoted B(FeP)x, and the corresponding chemical compositions in wt.% oxides are reported in Table 1. One part of the mixtures is devoted to differential thermal analysis and enthalpy measurements. The other part is slowly heated between 300 and 1000 °C by steps of 100 °C. Between each heat treatment, the products are reground and homogenized in presence of ethanol. Finally, the mixtures are pelletized, heated at 1400 °C during 24 h and rapidly quenched under air atmosphere.

The reactions of decarbonation and calcium silicates formation are observed by differential thermal analysis from room temperature to 1400 °C, at a constant rate of 10 °C min^{-1} under air atmosphere. The sample's masses used are in the range 300–400 mg.

Enthalpy variations are measured by isothermal calorimetry using a high-temperature Tian Calvet calorimeter. The sensors consist of two thermopiles constituted by hundreds of thermocouples Pt/Pt–Rh 13% [28]. Samples of about 30 mg are dropped at ambient temperature into the calorimetric cell, which is brought at various successive temperatures. At each temperature, the enthalpy variation is determined by time integration of the instantaneous heat flux over the whole duration of the occurring phenomenon. The atmosphere is argon. The calorimeter is standardized by drops of α alumina provided by the U.S. NBS laboratory [29], the enthalpy variations of which between ambient and experimental temperatures are well known.

The synthesized solid solutions at 1400 °C are analyzed by XRD using a D-5000 diffractometer at the Cu K_α radiation. Free lime in the final products is determined by the classical ethylene glycol method [30]. Finally, the textures of the final products are examined by SEM on gold metallized powders.

3. Results

3.1. Differential thermal analysis

The thermograms corresponding to the mixtures for $x=0$ to 0.20 are reported in Fig. 1.

A double endothermic peak at 150 °C is only observed for the doped samples, the importance of which increases as the dopant concentrations increase. It is attributed to the $(NH_4)_2HPO_4$ decomposition [31]. The DTA thermogram realized on pure $(NH_4)_2HPO_4$ confirms this observation. The endothermic peak, located around 569 °C, is relative to the quartz (β) → quartz (α) transition [1,9].

The main endothermic effect is attributed to the decarbonation reaction the characteristic temperatures, which are reported in Table 1 and plotted in Fig. 2. The onset temperature of the calcium carbonate decomposition decreases as the concentrations of Fe_2O_3 and P_2O_5 increase. For all the concentrations, the peak area that corresponds to nearly the same energy is almost identical, but its maximum decreases with the dopant concentration. The relative kinetics of the reactions becomes thus lower.

An exothermic effect is observed after the decarbonation reaction and goes up to 1400 °C for the B(FeP)0 and B(FeP)0.05 starting mixtures. For $x=0.10$ and 0.20, this effect ends at 1350 °C.

An endothermic effect occurs at around 1420 °C and is especially evident for the $x=0.10$ and 0.20 compositions. It may correspond to a partial fusion of the sample.

Table 1
Chemical compositions (wt.% oxide) and specific temperatures of the decarbonation step (reported from DTA curves) of the B(FeP)x starting mixtures

B(FeP)x samples	CaO	SiO_2	Fe_2O_3	P_2O_5	Onset temperature	Maximum temperature peak	Final temperature
B(FeP)0	65.12	34.88	0.00	0.00	709	898	920
B(FeP)0.05	62.25	33.34	2.33	2.07	685	889	914
B(FeP)0.10	59.34	31.79	4.69	4.17	665	884	909
B(FeP)0.20	53.42	28.62	9.50	8.45	624	884	908

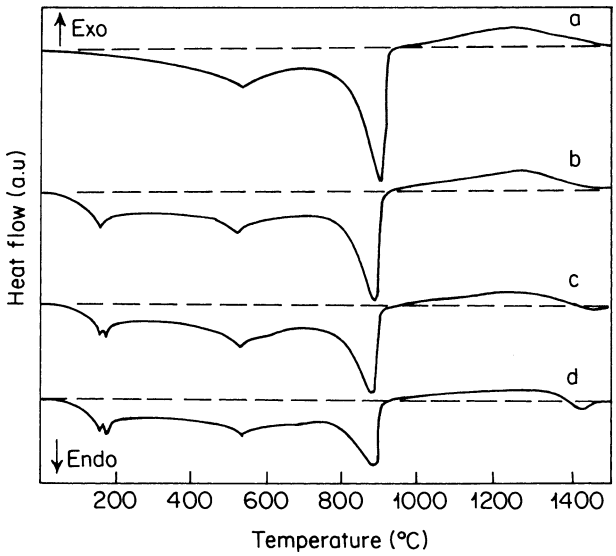

Fig. 1. DTA thermograms of starting samples: (a) B(FeP)0, (b) B(FeP)0.05, (c) B(FeP)0.10 and (d) B(FeP) 0.20.

It is the highest for the iron–phosphorus-rich compositions and is likely due to the flux effect of the iron oxide. This effect, which is added to the exothermic effect, lowers the maximum temperature of the previous exothermic reaction.

3.2. Enthalpimetry

The enthalpy variations of starting mixtures B(FeP)x at the temperatures ranging 683–957 °C are reported in Table 2 and plotted in Fig. 3.

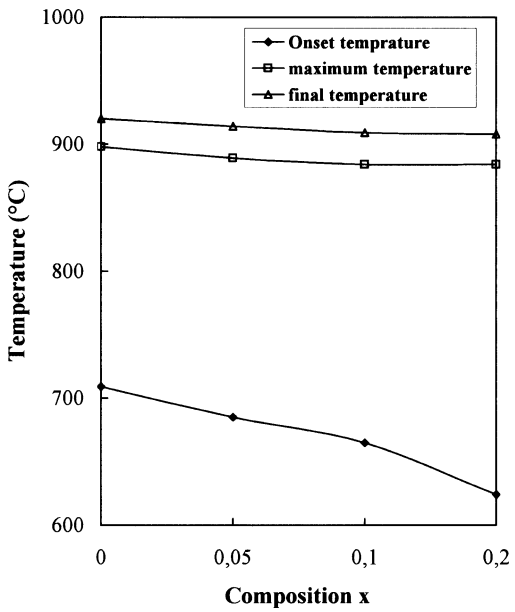

Fig. 2. Specific temperatures of decarbonation step as a function of the composition x of the B(FeP)x starting samples.

In the pure sample B(FeP)0, the decomposition reaction of $CaCO_3$ starts around 734 °C and goes up to 957 °C. The same evolution is observed for the B(FeP)0.05 sample. For the B(FeP)0.10 and B(FeP)0.20 samples, the decarbonation starts under 734 °C.

Around 835 °C, the enthalpy variations decrease gradually with the increase of x. The lower measured value (1930.7 J/g) corresponds to the B(FeP)0.20 starting mixture. At 957 °C, they seem to be almost constant with a slow minimum at $x = 0.05$.

After each set of drop enthalpy measurements, the powders resulting from the reactions in the calorimeter, at 957 °C, are analyzed by XRD. Taking into account that the whole experiment duration is for each set of measurement of about 10 h, it can be considered that the analyzed phases are the results of almost complete reactions. The corresponding patterns are given in Fig. 4. The B(FeP)0 sample is essentially constituted by the CaO and SiO_2 oxides. SiO_2 is present in two forms: α quartz and α cristobalite. Very weak peaks of the CS and C_3S_2 phases are also detected. For the $x = 0.05$ composition, the same products after reaction are observed. The analysis of the B(FeP)0.10 sample shows the onset crystallization of C_2S under the β form. Moreover, a decrease in the concentrations of CaO and SiO_2 and an increase in those of CS and C_3S_2 are observed. A small

Table 2
Enthalpy variations (J/g) of the B(FeP)x starting mixtures versus temperature

B(FeP)x samples	Temperature (°C)			
	683	734	835	957
B(FeP)0	741.2	846.4	2202	3196.3
B(FeP)0.05	767.5	862.1	2189.8	3056.3
B(FeP)0.10	831.9	972.9	2174.8	3154.7
B(FeP)0.20	959	1230.4	1930.7	3200.4

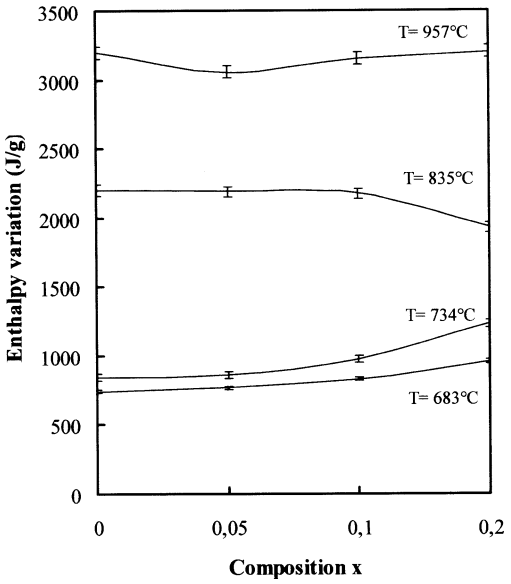

Fig. 3. Enthalpy variations versus of the composition x of the B(FeP)x starting mixtures.

quantity of the ferrite phase $CaO.Fe_2O_3$ (CF) is also identified. For the B(FeP)0.20 sample, this later phase appears instead of the β-C_2S.

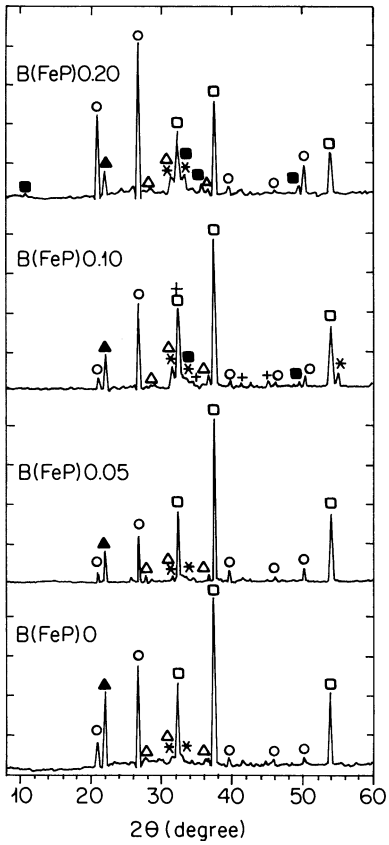

Fig. 4. XRD patterns of B(FeP)x starting materials, heated in the calorimeter at 957 °C. Symbols: □ CaO, ○ SiO_2 (quartz α), ▲ SiO_2 (cristobalite α), ∗ C_3S_2, + β-C_2S, Δ CS and ■ CF.

Table 3
Crystalline phases identified by X-ray diffraction in the B(FeP)x-synthesized samples at 1400 °C

B(FeP)x samples	γ-C_2S	β-C_2S	α′-C_2S	α-C_2S
B(FeP)0	+	+++	–	–
B(FeP)0.05	–	+++	–	–
B(FeP)0.10	–	–	+++	–
B(FeP)0.20	–	–	o	+++

+++ = abundant; ++ = medium; + = little; o = traces; – = absent.

3.3. High-temperature mineralogy

The identified crystalline phases appearing after a heat treatment up to 1400 °C are semiquantitatively estimated for the B(FeP)x samples. The results are given in Table 3, and the corresponding X-ray patterns are reported in Fig. 5.

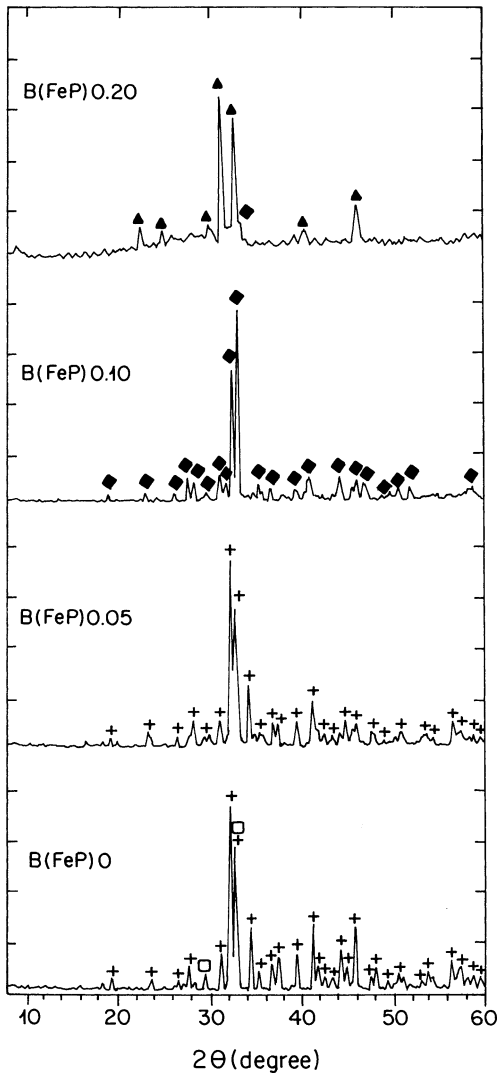

Fig. 5. XRD patterns of B(FeP)x-synthesized samples at 1400 °C. Symbols: □ γ-C_2S, + β-C_2S, ◆ α′-C_2S and ▲ α-C_2S.

In the pure sample B(FeP)0, the most predominant phase is β-C_2S. A little quantity of γ-C_2S is also identified. In the B(FeP)0.05 sample, only the allotropic form β-C_2S is stabilized. On the B(FeP)0.10 pattern, only the α′-C_2S phase is observed. For the B(FeP)0.20 sample, the high-temperature polymorph α-C_2S is mostly stabilized with traces of α′-C_2S.

3.4. Free lime analysis

The free-lime quantity is determined chemically in the solid solutions treated at 1400 °C. No free lime is detected in the Fe_2O_3 and P_2O_5 doped samples. In the nondoped composition, the quantity of free lime is measured at 0.45 wt.%.

3.5. SEM observations

The B(FeP)0 and B(FeP)0.10 samples are observed by SEM. The corresponding micrographs are reported, respectively, in Figs. 6 and 7.

The micrograph of B(FeP)0 presents only belite with a mean grain size of 2–3 μm. These grains exhibit rounded or oval forms, as it has been already observed by other authors [15,32]. The belite grains are joined, present a random dispersion and do not exhibit microcracks on their surfaces.

α′-C_2S crystals, the size of which do not exceed 2–4 μm, are observed in the B(FeP)0.10 corresponding micrograph. Indeed, the crystal surface presents irregular forms with microcracks as grain boundaries. These observations are in agreement with the conclusions of Weisweiler et al. [18]. These authors have also observed grain boundaries in iron-doped belite.

A vitreous phase surrounding the grain of belite is observed in the micrograph of the B(FeP)0.10 sample. An annealing at 1000 °C of this sample exhibits the crystallization of that glassy phase identified by XRD as CS_2. It was already reported in the literature that the presence of Fe_2O_3 in a $CaO–SiO_2$ system could induce similar observation [18].

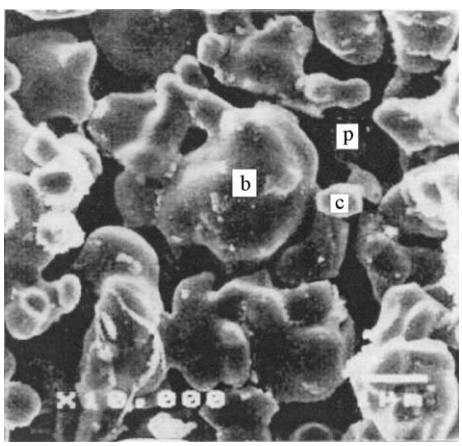

Fig. 6. Micrograph of the B(FeP)0 sample heated at 1400 °C. b—belite grain (β-C_2S), p—pore of the structure, c—free CaO.

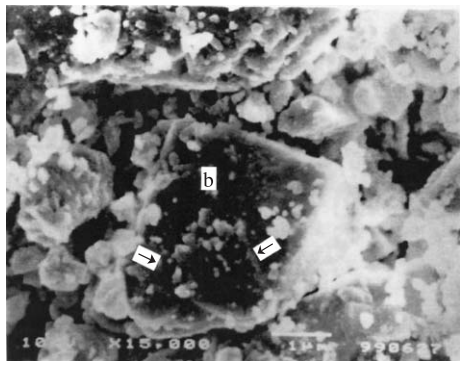

Fig. 7. Micrograph of B(FeP)0.10 sample heated at 1400 °C. b—belite crystallite (α′-C_2S); → grain boundaries.

4. Discussion

The Fe_2O_3 and P_2O_5 additions induce a reduction of the onset decarbonation temperature from 709 to 624 °C, respectively, for Fe_2O_3/P_2O_5 ratios ranging from 2.33/2.07 to 9.50/8.45 wt.% in $CaO/SiO_2 \approx 2$ mixtures. In the study of Qotaibi et al. [7], it was already observed that the increase of the Cr_2O_3 and P_2O_5 quantities in $CaO/SiO_2 \approx 2$ mixtures leads to a decrease of the onset temperature of $CaCO_3$ decomposition from 711 to 647 °C. Ahluwalia and Mathur [9] have shown that the presence of the transition element oxides Cr_2O_3, TiO_2 and Mn_2O_3 in a $CaCO_3–SiO_2$ (2:1) system decreases the onset temperature of decarbonation when the concentrations of additives increase from 0.1 to 1 wt.%. The study carried out by Agarwal et al. [33] on the simultaneous effect of $CaCl_2$ and $MgCO_3$ on the decarbonation reaction showed that the 2.2 wt.% Cl and 2.2 wt.% MgO addition leads to the decrease in decarbonation temperature of about 48 °C. It can be compared with the present study where the temperature decrease is about 85 °C.

The exothermic effect observed after the end of the B(FeP)*x* samples decarbonation is mainly attributed to the crystallization of the CS, C_3S_2 and C_2S phases [1,8,9]. Indeed, the formation of C_2S beyond 1000 °C results from a reaction between the intermediate phases CS, C_3S_2 and CaO [1].The reaction between the CaO produced from the decarbonation of $CaCO_3$ and SiO_2 occurs in solid state by the diffusion of the Ca^{2+} ions through the layer formed by the products of the $CaO–SiO_2$ reaction around the silica grain. C_3S_2 and CS are preferentially formed on the core of the SiO_2 grains and C_2S at the open interface.

The increase of the enthalpy variations at 734 °C of doped compositions is in agreement with the DTA results, which shows that the endothermic reaction of decarbonation starts below 734 °C for higher iron and phosphorus oxides contents. The enthalpy variations at 835 °C apparently

decrease versus x, and a minimal value is observed for $x = 0.20$. At the highest temperature, the enthalpy variation remains also apparently constant within the error margin. The mean experimental scatter increases with the temperature. The values for the 683 and 734 °C are normal for this kind of experiments; both the others become abnormal all the more great because the temperature is high. Such a large scatter occurs when the heat production in the cell is not reproducible. It is especially the case at 957 °C, where the kinetics of the exothermic reactions of formation of the CS, C_3S_2 and C_2S silicates [1,8,9] are very low because they involve matter diffusion for completion. During the calorimetric observation (about 20 min), the reaction cannot be completely achieved. The DTA measurements show that the maximum rate of these exothermic reactions is at least around 1200 °C, which lies 250 °C over the highest temperature for the enthalpy measurements. All these consistent observations lead to avoid drawing precise conclusions from these last results. Nevertheless, a tendency to a decrease of the enthalpy variation (about 10%) for high values of x is credible.

The X-ray analysis of the B(FeP)0 to B(FeP)0.20 samples heated at 957 °C in the calorimeter shows that the Fe_2O_3 and P_2O_5 oxides promote the crystallization of the intermediate phases CS, C_3S_2 and, consequently, β-C_2S. This observation is consistent with the fact that the Fe_2O_3 oxide transforms the quartz crystals into very reactive cristobalite at temperature ranging from 800 to 1000 °C [6]. This last phase then reacts easily with the CaO of the raw mixture to give the calcium silicate phases.

The present mineralogical study of the B(FeP)x samples shows that at room temperature the iron and phosphorus doped C_2S is stabilized in the β, α′ and α forms for additions less than 9.50 wt.% Fe_2O_3 and 8.45 wt.% P_2O_5. The evolution of the allotropic forms of belite versus x, for $0.05 \le x \le 0.20$, agrees with previous studies on the effect of P_2O_5. The authors have shown that the increase of P_2O_5 concentrations induces the stability of C_2S forms according to the sequence $\beta \rightarrow \alpha' \rightarrow \alpha$ [7,34].

In the XRD pattern, the peaks of synthesized β, α′ and α iron–phosphorus-doped dicalcium silicate occur at higher 2θ values compared with the pure C_2S forms showed in the literature by several authors [6,19]. Thus, in the structure of C_2S, the iron ions can be located in the octahedral sites in substitution of calcium ions [35] and phosphorus, as PO_4 entities can replace the SiO_4 groups [25–27]. The ionic radius of Fe^{3+} (0.64 Å) and P^{5+} (0.35 Å) are, respectively, smaller than that of Ca^{2+} (0.99 Å) and Si^{4+} (0.42 Å) [36]. That induces a contraction of doped C_2S lattice.

In this work, the β-C_2S phase is the only stabilized phase at the 2.33 wt.% Fe_2O_3 and 2.07 wt.% P_2O_5 concentrations. Matkovich and Young [21] have found that the addition of 1.42–2.27 wt.% P_2O_5 stabilizes both the β and α′ forms. In the other hand, the Fe_2O_3 addition induces the only formation of the β form [35]. Consequently, for the B(FeP)0.05 composition, the presence of Fe_2O_3 inhibits the stabilizing effect of P_2O_5 on the α′-C_2S formation. Beyond this composition, the phosphorus effect is predominant.

The absence of free lime in the C_2S-doped solid solutions is due to the known flux effect of Fe_2O_3 and P_2O_5 oxides in clinkerisation reactions [17,20]. These oxides lead to the decrease of the melting point of the mixtures and, thus, the increase of the liquid phase amount, which make easier the diffusion of CaO in SiO_2 grains.

The SEM observations of the B(FeP)0 and B(FeP)0.10 samples show that the iron and phosphorus incorporations induce microcraking at grain boundaries on the grain surface of dicalcium silicate. This is consistent with the increase of the hydraulic reactivity of C_2S that has been already reported by several authors [37–39].

5. Conclusion

In $CaCO_3$–SiO_2 (2:1) reacting mixtures, the onset temperature of decarbonation decreases with Fe_2O_3 and P_2O_5 additions of, respectively, less than 9.50 wt.% and 8.45 wt.%. The corresponding reduction of temperature decarbonation is about 85 °C. At the temperature of about 835 °C, the energy consumption during the decomposition reaction of $CaCO_3$ decreases about 12%, with the increase of iron and phosphorus concentrations. The mineralogical analysis of the synthesized solid solutions $(Ca_{2-2x}Fe_x\square_x)(Si_{1-x}P_x)O_4$ shows the formation of β, α′ and α belite modifications. For the only (Fe_2O_3 2.33–P_2O_5 2.07 wt.%) composition, the presence of iron oxide inhibits the formation of the α′ form, which will have to be stabilized by the phosphorus oxide. Beyond this composition, the phosphorus effect is predominant.

Acknowledgements

The authors would like to acknowledge Dr. H. Bros for help in the calorimetric measurements.

References

[1] F. Ayed, Contribution à l'étude des phénomènes thermiques lors de la clinkérisation de crus de ciment Portland, thesis, Univ. Provence, Marseille, France, 1991.
[2] V. Johansen, N.H. Christensen, Rate of formation of C_3S in the system $CaO–SiO_2–Al_2O_3–Fe_2O_3–MgO$ with addition of CaF_2, Cem. Concr. Res. 9 (1979) 1–6.
[3] I.F. Xiuji, H. Yufeng, Research on an early strength cement containing high content of iron, in: Finep (Ed.), 8th ICCC, Rio de Janeiro, Brazil, vol. 2, 1986, pp. 285–292.
[4] G. Moir, F.P. Glasser, Mineralisers modifiers and activators in the clinkering process, 9th ICCC, New Delhi, India 1 (1992) 125–152.
[5] S. Dagen, C. Welqing, H. Qixiu, M. Huo, Z. Liqiang, Effect of SO_3 on mineral formation and properties of clinkers, 9th ICCC, New Delhi, India 2 (1992) 322.
[6] H.F.W. Taylor, Cement Chemistry, Thomas Telford Publishing, London, 1997.

[7] Z. Qotaibi, A. Diouri, A. Boukhari, J. Aride, J. Rogez, R. Castanet, Synthesis and thermal study of chromium–phosphorus doped dicalcium silicate, World Cem. Res. 26 (1999) 77–80.
[8] I.P. Saraswat, V.K. Mathur, S.C. Ahluwalia, Thermal decomposition and phase transformation studies of $CaCO_3$–SiO_2 (2:1) system in presence of sodium and potassium carbonate, in: FINEP (Ed.), 8th ICCC, Rio de Janeiro, Brazil, vol. 2, 1986, pp. 162–166.
[9] S.C. Ahluwalia, V.K. Mathur, Thermal studies on the effect of transition metal oxides on the kinetics of formation and stabilization of β-dicalcium silicate, in: FINEP (Ed.), 8th ICCC, Rio de Janeiro, Brazil, vol. 2, 1986, pp. 40–45.
[10] My.Y. Benarchid, A. Diouri, A. Boukhari, J. Aride, R. Castanet, J. Rogez, Thermal study of chromium–phosphorus doped tricalcium aluminate, Cem. Concr. Res. 31 (2001) 449–454.
[11] D.K. Smith, A. Majumdar, F. Ordway, The crystal structure of γ-dicalcium silicate, Acta Crystallogr. 18 (1965) 787–795.
[12] W. Eysel, T. Hahn, Polymorphism and solid solution of Ca_2GeO_4 and Ca_2SiO_4, Z. Kristallogr, Bd. 31 (1970) 322–341.
[13] I. Jelenic, A. Bezjak, M. Bujan, Hydration of B_2O_3-stabilized α′- and β-modifications of dicalcium silicate, Cem. Concr. Res. 8 (1978) 173–180.
[14] I.F. Xiuji, Y. Peiyu, Effect of the states of chromium ion on the colour characteristics of doped β-C_2S, Adv. Cem. Concr. Res. 3 (10) (1990) 85–88.
[15] R. Trettin, G. Oliew, C. Stadelmann, W. Weiker, Very early hydration of dicalcium silicate–polymorphs, Cem. Concr. Res. 21 (1991) 757–764.
[16] K. Rajczyk, Hydraulic activity of low temperature dicalcium orthosilicate modified by BaO addition, in: H. Justnes (Ed.), 10th ICCC, Gothenburg, Sweden, vol. 2, 1997, pp. 45–49.
[17] R.M. Herath Banda, F.P. Glasser, Role of iron and aluminum oxides as fluxes during the burning of Portland cement, Cem. Concr. Res. 8 (1978) 319–324.
[18] W. Weisweiler, E. Osen, M. Lamperle, Effect of Fe_2O_3 and Al_2O_3 admixtures on the reaction kinetic between CaO- and SiO_2-powder compact, in: Finep (Ed.), 8th ICCC, Rio de Janeiro, Brazil, vol. 2, 1986, pp. 83–88.
[19] M. Regourd, Crystal chemistry of Portland cement phases, in: P. Barnes (Ed.), Structure and Performance of Cement, Applied Science, London, 1983, pp. 109–138.
[20] R.W. Nurse, The effect of phosphate on the constitution and hardening of Portland cement, J. Appl. Chem. 2 (1952) 708–716.
[21] B. Matkovich, J.F. Young, Dicalcium silicates doped with phosphates, in: Finep (Ed.), 8th ICCC, Rio de Janeiro, Brazil, vol. 2, 1986, pp. 276–281.
[22] W. Gutt, High temperature phase equilibria in the system $2CaO.SiO_2$–$3CaO.P_2O_5$–CaO, Nature 197, 1963 (January 12) 142–149.
[23] W. Gutt, Manufacture of Portland cement from phosphatic raw materials, 5th ICCC, Tokyo, Japan 1 (1968) 93–105.
[24] L. Halicz, Y. Nathan, L. Ben-Dor, The influence of P_2O_5 on clinker reactions, Cem. Concr. Res. 14 (1) (1984) 11–18.
[25] A. Diouri, A. Boukhari, J. Aride, F. Puertas, T. Vazquez, Formation d'hydroxyapatite $Ca_5(PO_4)_3OH$ en milieu silicaté, Mater. Constr. 45 (236) (1994) 5–13.
[26] A. Diouri, A. Boukhari, J. Aride, F. Puertas, T. Vazquez, Research of the lime rich portions of the CaO–SiO_2–P_2O_5 system, Mater. Constr. 45 (237) (1995) 3–13.
[27] A. Diouri, A. Boukhari, J. Aride, F. Puertas, T. Vazquez, Elaboration of α'_L-C_2S form of belite in phosphatic clinker. Study of hydraulic activity, Mater. Constr. 48 (249) (1998) 23–32.
[28] R. Castanet, F.P. Sorrentino, Study of clinkering reactions by high temperature isothermal calorimetry, in: Finep (Ed.), 8th ICCC, Rio de Janeiro, Brazil vol. 2, 1986, pp. 36–39.
[29] G. Uriano, Standard reference materials 720, Synthetic Sapphire, Nat. Bur. Stand, US. Depart. Commerc, Washington DC, 1986.
[30] P. Arjounan, A. Kumar, Rapid techniques for determination of free lime and free magnesia in cement clinker and Portlandite in hydrates, Cem. Concr. Res. 24 (2) (1994) 343–352.
[31] R.C. Weast, Handbook of Chemistry and Physics, CRC Press, 58th Edition, Cleveland-Ohio, 1977–1978.
[32] K. Nabih, Caractérisation et traitements thermiques des schistes bitumineux des sous-couches R de Tarfaya sons différentes atmosphères (N_2, He, air et vapeur d'eau). Utilisation des cendres dans la production du ciment, Thesis, Univ Mohamed V, Rabat, Maroc., 1997.
[33] R.K. Agarwal, S.V. Paralkar, A.K. Chatterjee, Chloride salts as reaction medium for low temperature clinkerisation—a probe into alinite technology, in: Finep (Ed.), 8th ICCC, Rio de Janeiro, Brazil, vol. 2, 1986, pp. 327–333.
[34] A. Diouri, A. Boukhari, J. Aride, F. Puertas, T. Vasquez, Stable Ca_3SiO_5 solid solution containing manganese and phosphorus, Cem. Concr. Res. 27 (8) (1997) 1203–1212.
[35] G. Lai, T. Nijiri, K. Nakano, Studies of stability of β-Ca_2SiO_4 doped by minor ions, Cem. Concr. Res. 22 (1992) 743–754.
[36] R.D. Shannon, Acta Crystallogr., A 32 (1976) 751.
[37] Y. Nanru, Z. Hua, Z. Belqian, Study on hydraulic reactivity and structural behaviour of very active β-C_2S, 9th ICCC, New Delhi, India 2 (1992) 285–291.
[38] Z. Lu, K. Tan, Activity of β-C_2S under different sintering conditions, Cem. Concr. Res. 27 (8) (1997) 989–993.
[39] F. Xiuji, M.S. Long, L. Shi-Zong, D. Qin-Jun, H. Cong-Yun, Investigation on doped β-C_2S with positron annihilation, in: Finep (Ed.), 8th ICCC, Rio de Janeiro, Brazil, vol. 2, 1986, pp. 128–133.